Magnetic Nanoparticle Formulations as MRI Contrast Agents: A Review

Abstract: Magnetic nanoparticles have been developed for use in a number of interesting biological applications, including contrast agents in magnetic resonance imaging (MRI), drug delivery vectors, and mediators for converting electromagnetic energy to heat. Massive attempts have been made to create magnetic nanoparticles for MRI contrast agents. Herein, we show the synthesis methods for perpetration of iron oxide nanoparticles with surface modifications and also include characterization techniques used for size, surface and magnetic properties detection. A brief discussion on magnetic nanoparticles, toxicity and angiogenesis activity is included. In this review, we discuss to develop iron oxide based nanoparticles (NPs) formulations, preferably aqueous dispersions which are superparamagnetic, stable and biocompatible with suitable cell lines, for application as *T2* MRI contrast agents with better *r2* relaxivity.

Introduction

Nanoparticles (NPs) are more reactive than bulk materials due to their high surface to volume ratio. Magnetic NPs form a class of NPs which can be manipulated by small magnetic fields. The synthesis of uniformly sized magnetic NPs has been intensively pursued because of their broad applications including magnetic storage media, ferrofluids, magnetic resonance imaging (MRI), magnetically guided drug delivery and catalysts for the growth of carbon nanotubes [1-3]. Studies on magnetic NPs are being intensively pursued not only for fundamental scientific interest but also for their novel application capability arising due to their unique physical and chemical properties [4]. The superparamagnetic iron oxide nanoparticles (SPIONs) has a high potential in biomedical applications such as cellular therapy, tissue repair, drug delivery, magnetic resonance imaging (MRI), hyperthermia, etc. [5-7], since they are considered less toxic than their metallic counterparts. For these applications, the NPs must have combined properties of high magnetic saturation, size less than 50 nm, biocompatibility, pH neutral, chemical stability and agglomeration free. The main problem with NPs is their fast agglomeration and to avoid this, these NPs are coated with various polymer such as dextran, chitosan, polyethylene glycol (PEG), polyvinyl alcohol [8-11]. Recently, iron oxide NPs with different coatings have been widely investigated, due to their desirable magnetic properties in biomedicine and bioengineering fields. Also, these materials should have low toxicity and high biocompatibility. Toxicity of NPs on the human health is one main feature for successful application of NPs in medicine. Recently, the cytotoxicity effects of iron oxide coated with thiol containing hydrophilic ligands has found to be non-toxic in human lymphocytes while nitric oxide releasing iron oxide NPs are found to be toxic in human

lymphocytes; hence the latter is used in the treatment of tumours cells [12], Fe_3O_4 NPs coated with chitosan are biocompatible with human osteoblast cells [13], sodium oleate coated Fe_3O_4 do not possess any toxic effect on 3T3 cells [14]. The presence of surface coating is found to render good aqueous dispersion stability, less agglomeration and excellent biocompatibility, hence makes them suitable candidate for biomedical applications.

Figure 1. Applications of Magnetic Nanoparticles.

Magnetism in ultrafine particles:

Magnetism in materials at nanoscale is very fascinating. Generally, the properties of nanomaterials differ substantially from the bulk counterparts.

Single domain particle:

In a large body there could be minimum domain size below which energy cost of domain formation exceeds the benefits from decreasing magnetostatic energy. This implies that a single particle of size comparable to the minimum domain size would not break up into domains.

Qualitatively it is observed that if a particle is smaller than that about 100 nm, a domain wall simply can't fit inside it, resulting in single domain particles. A single domain particle has high magnetostatic energy, but no domain wall energy, whereas a multidomain particle has lower magnetostatic energy but higher domain wall energy. Before application of an external field, the magnetization of a single domain particle lies along an easy direction which is determined by the shape and magnetocrystalline anisotropies. When an external field is applied in the opposite direction, the particle is unable to respond through the hard direction, to the new easy direction [16-19].

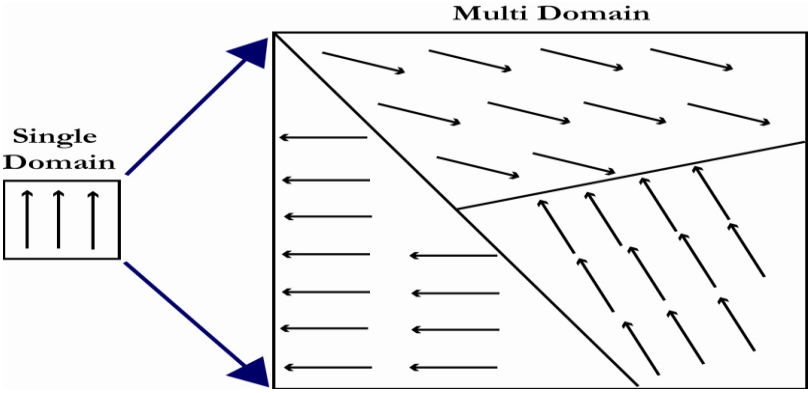

Figure 2. The effect of increasing particle size, by going from a small single domain particle to the large particle results in multi domain materials with domain boundaries.

Superparamagnetism:

A very small ferromagnetic or antiferromagnetic particles can behave, below a so called blocking temperature, like a giant magnetic moment (or macro-spin). Applying a magnetic field will then induce magnetization which follows a H/T law given by *Langevin function*, since the situation is that of the classical limit of infinite spins.

However it should be noticed that the blocking temperature varies with the time scaleof the measurement, and with the volume of the particle, because the transition of the particle from a blocked state (with a magnetic moment rigidly directed along a given direction) toward the *superparamagnetic state* is a relaxation phenomenon. Thus, at room temperature, fine particles can seem to be superparamagnetic when their magnetization is measured with the classical extraction technique (duration of the experiment of the order of a second) while a neutron

diffraction experiment will see them “blocked” as the neutron-spin interaction time is very short [15].

It was L. Neel who developed in 1949 the superparamagnetism theory (without using the term of superparamagnetism) for ferromagnetic fine particle [20], and extended it 1961 to antiferromagnetic fine particles [21]. These two basic articles are reproduced in his collected scientific works [22].

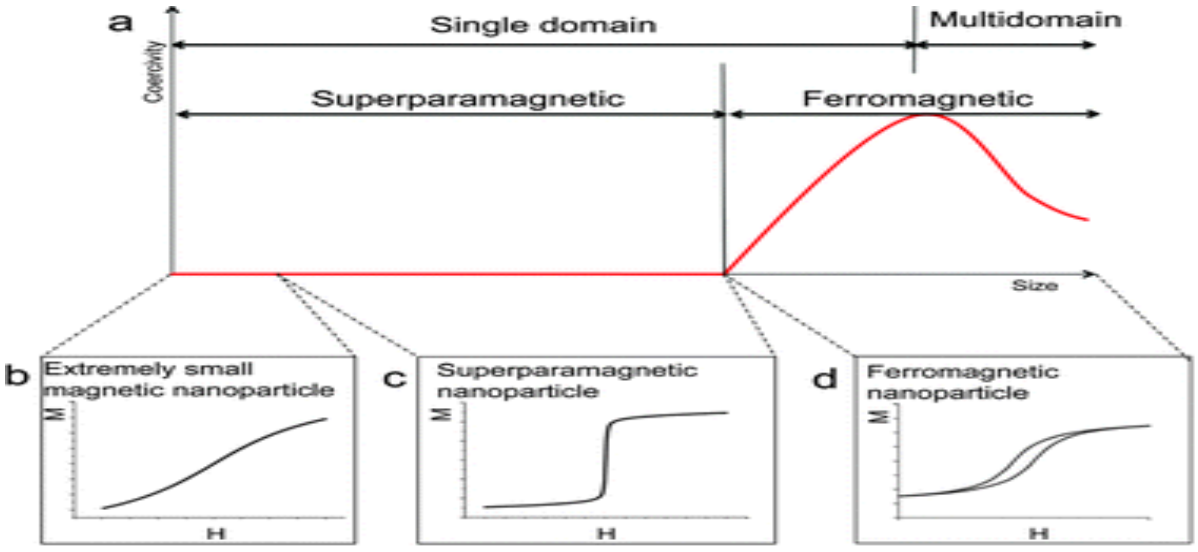

Figure 3. Size dependent variation of Hysteresis magnetization of fine particles.

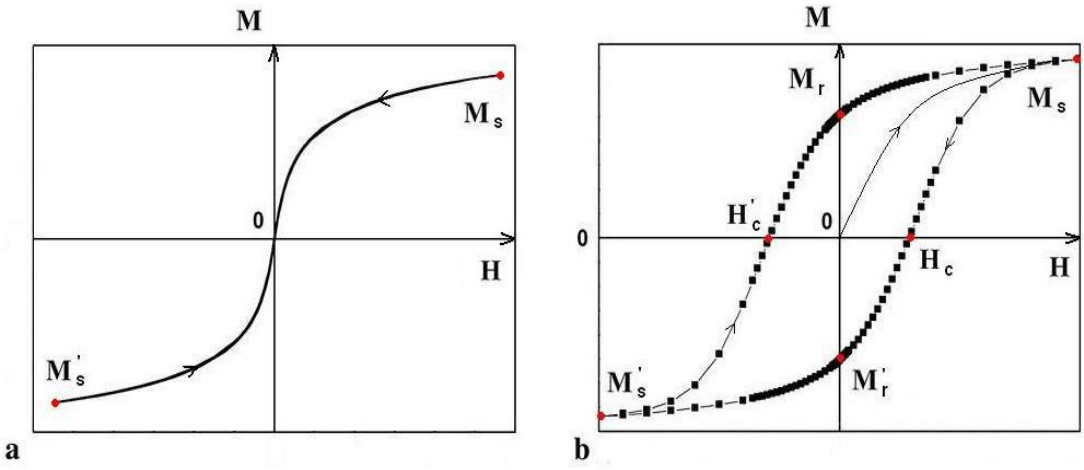

Figure 4. Comparing magnetization curves of (a) superparamagnetic and (b) ferromagnetic materials.

Synthesis techniques:

Nanomagnetic materials are very sensitive to processing conditions and impurity levels because small contents of non-magnetic impurities can alter the properties substantially. Hence the choice of technique for the preparation of metallic NPs and their composites are very vital. For example iron oxide NPs prone to oxidation even at room temperature in open atmosphere. A special care is needed for the synthesis of metallic NPs. Moreover, it is too difficult to prepare a nanocomposite comprising a metal and an oxide. The development of a high purity material is very crucial for investigation of involved physical properties. There are many methods to synthesize iron oxide NPs: sol gel, thermal decomposition, water–in-oil emulsion, polyol, gas deposition, co-precipitation, hydothermal and others. Every method possess specific performance procedure and conditions, and of course NPs of different properties (shape, average size, size distribution, crystallinity, magnetic NPs,dispersibility, etc). There are two approaches for synthesis of nanomaterials. They are Top-down approach and Bottom-up approach. The magnetic NPs are mostly synthesized by bottom-up approach method. In this work two methods with high product quality/synthesis difficulty ratio will be compared. These routes are co-precipitation and thermal decomposition. The coating of iron oxide NPs is done by stirring, heating and sonication.

Co-precipitation method:

In chemistry, co-precipitation is the process in which precipitate of substances normally soluble under the conditions employed is achieved [23]. There are three main mechanisms of co-precipitation: inclusion, occlusion, and adsorption [24]. An inclusion occurs when the impurity occupies a lattice site in the crystal structure of the carrier, resulting in a crystallographic defect; this can happen when the ionic radius and charge of the impurity are similar to those of the carrier. An adsorbate is an impurity that is weakly bound (adsorbed) to the surface of the precipitate. An occlusion occurs when an adsorbed impurity gets physically trapped inside the crystal as it grows. Co-precipitation is used as a method of magnetic NPs synthesis. [25]. Co-precipitation is a facile and convenient way to synthesize iron oxides (either Fe_3O_4 or γ-Fe_2O_3) from aqueous Fe^{2+}/Fe^{3+} salt solutions by the addition of a base under inert atmosphere at room temperature or at elevated temperature. The size, shape, and composition of the magnetic NPs depends on the type of salts used (e.g. chlorides, sulphates, nitrates), the Fe^{2+}/Fe^{3+}ratio, the reaction temperature, the pH value and ionic strength of the media [25]. In recent years, co-precipitation approach has been used

extensively to produce ferrite NPs of controlled sizes and magnetic properties [26-29]. Co-precipitation reaction involves simultaneous occurrence of nucleation, growth, coarsening, and/or agglomeration process. Co-precipitation reaction exhibits the following characteristics: (i) the products are generally insoluble species formed under the condition of high supersaturation; (ii) nucleation is a key step and a large number of small particles will be formed; (iii) secondary processes such as Oswald ripening and aggregation, dramatically affect the size, morphology and properties of the end products; (iv) the supersaturation conditions necessary to induce precipitation are usually the result of a chemical reaction

$X\ A_{y+}\ (aq.) + Y\ B_{x-}\ (aq.) \leftrightarrow A_xB_y\ (S)$;

where X = molar concentration of A, Y = molar concentration of B, y_+ = ionic state of A,

x_- = ionic state of B

Particle size of the co precipitated material is strongly dependent on the pH of the precipitation medium and molarity of the starting precursors. Consequently, control over the size can be easily achieved. The reaction and transport rates are affected by the concentration of the reactants, temperature, pH, the order in which the reagents are added to the solution and mixing. The structure and crystallinity of the particles can be influenced by reaction rates and impurities. Particle morphology is influenced by factors such as supersaturation, nucleation and growth rates. At low supersaturation, the particles are small, compact and well-formed and the shape depends on crystal structure and surface energies. At high super saturation levels, large and dendritic particles are formed. Co-precipitation method offers distinct advantages like simple and rapid preparation, easy control of particle size, composition and various possibilities to modify the particle surface state and overall homogeneity over other preparative methods. Co-precipitation is a facile and convenient way to prepare colloidal magnetic NPs [25], and the reactions scale well to produce high amount of particles: ~10 g with yields around 85% [30-33]. In the present investigation, NPs of iron oxide were synthesized by a wet chemical route using iron chloride as a precursor. Ammonia solution and sodium hydroxide was used as the reducing agent. The reaction was done at room temperature. Similarly, for synthesis of coated NPs, the required coating agents like curcumin, dextran, PEG- 6000 were added after the precipitate formation using ammonia solution as reducing agent.

Thermal decomposition method:

The thermal decomposition of organometallic precursors method has been widely used in iron oxide based NPs synthesis. Some organic iron compounds Ferric acetylacetonate [$Fe(acac)_3$], iron oleate [$Fe(oleate)_3$], iron pentacarbonyl [$Fe(CO)_5$] are decomposed at high temperature inside the non-polar boiling solvent with the presence of capping agent [34]. Most of the precursors used in this method are toxic and not friendly to environment. This synthesis method can lead to high-quality monodispersed iron oxide NPs, which usually requires relatively higher temperature and a complicated operation. Narrow size distribution high crystallinity and shape control are the attributes of this route [35]. The precursor is heated upto the boilng point of boiling solvent with a constant heating rate and kept at this temperature for the desired time. Narrow size distribution is obtained due to feature of the nucleation and growth mechanism during decomposition- these processes occur at different temperatures and can be well-separated. The nucleation starts at approximately 200^{o} C 230^{o} C and the growth at 260^{o} C – 290^{o} C. The NPs are coated with capping ligand (fatty acids, hexadecylamine), it is not only the size adjustment instrument, but also colloidal stabilizer [36]. Prepared by this techniques NPs are hydrophobic (not soluble in water) and can stored in hexane, cyclohexane, toluene or other non-polar solvents. There are several ways to control size and shape of NPs. The size can be tuned by three factors: (i) temperature of the decomposition reaction (depends on boiling solvent), (ii) precursor/caping agent ratio, (iii) duration of the reaction after reaching the boiling point. Morphology of the NPs mostly influenced by the heating rate and precursor/boiling solvent volumetric ratio. Many different conditions of the experiment were investigated: changing the boiling solvent (di-n- hexyl ether) boiling point 228^{o}C, hexadecene (bp 274^{o} C), dioctyl ether (bp 294^{o}C) and octadecene (bp 317^{o}C); different amount of capping agent – oleic acid [37]. This method gives high quality NPs however the amount is quite low per one batch. One of the most significant difficulties of this route is to establish constant heating rate, especially in the range where the nucleation and growth occurs. “Green” synthesis with non toxic and environment friendly precursors (ferric chloride and sodium citrate, for example) is preferable [38]. This method gives high quality NPs, highly dispersible in water and non-toxic and also the yield is quite high per batch.

Sonication:

The study of sonication is concerned with understanding the effect of sonic waves and wave properties on chemical systems. Since acoustic waves have unique physical properties, the

corresponding atomic and molecular chemistry is unique as well. Sonication is concerned with study of chemical reactions powered by high frequency sound waves. Ultrasonic waves in liquid cause the formation of tiny bubbles that collapse within short time. It is believed that small cavities (~100 microns) which implode create tremendous heat and pressure, shock waves and particle accelerations. This process is called "cavitation" [39-41]. The ultrasonic power supply transforms line voltage to high frequency 20 kHz of electric energy. This electrical energy is transmitted to the probe where it is changed to mechanical energy. The vibrations from the probe are couples to and intensified by a titanium tip attached with it. The probe vibrates in a longitudinal direction and transmits this motion to the titanium tip immersed in the solution. Microscopic vapor bubbles that are formed momentarily can results in cavitation. After being created, these bubbles are filled with vapour and gas. Typically the bubbles in sonication are driven below their natural frequency at high pressure amplitudes, the bubbles undergo slow expansions and rapid, catastrophic collapse. The bubble compression is so violent that the gas in the bubble has been estimated (through computations and experiments) to reach temperature ~5000-8000 kelvin and pressure > 10,000 atmospheres on a nanosecond time scale. Heterogeneous sonochemistry occurs between liquid-liquid systems or solid-liquid systems [42-44]. Sonication, exposure to sound waves (In this work, sonication will exclusively mean irradiation of materials to high-intensity ultrasound), is used to mix homogeneously and modify the surface of powders of different constituents. An ultrasound sonicator was used for the preparation of coated iron oxide NPs.

Characterization:

The characterization techniques used for after synthesis of MNPs are as follows:

Surface morphology and coating layer thickness will be analyzed by Transmission and Scanning Electron Microscopy, equipped with an energy-dispersive x-ray spectrometer (EDS). Bright-field TEM (BFTEM) images, high-resolution TEM (HR-TEM) images, Fast Fourier Transform (FFT) image and selected area electron diffraction (SAED) patterns will also be recorded. These will provide morphological, structural, and compositional information of the SPIONs of different shapes, sizes and coatings. The structure characterization of SPIONs will be carried out in Bragg-Brentano (Θ-2Θ) configuration using X-ray diffraction (XRD) technique. Fourier Transform Infrared Spectroscopy (FT-IR) and Raman spectroscopy will be used to identify the eventual presence of chemical species in the SPIONs. DLS and Zeta potential measurements were carried

out for hydrodynamic size and stability of SPIONs. Magnetic measurements were done on a Quantum Design PPMS of 9T VSM for finding magnetic properties such as saturation magnetization, coercivity, blocking temperature and susceptibility.

Magnetic Nanoparticles in various biomedical studies:

Nanotechnology is a potential growing field as with immense application in the field of biomedicine. It is projected that production of NPs will increase from the estimated 300 tons produced today to 58,000 tons by 2020 [45]. Nanotechnology, in combination with biomedical developments, offers the promise of a revolutionary tool for the biomedical analysis [46]. More specifically nanotechnology may be translated into biomedicine thereby referring to treatment and curing of diseases at a molecular scale. The use of NPs (100nm and smaller) for delivery and diagnostics agents is at the forefront of projects in cancer treatment [47]. In vitro studies are becoming essential to substantiate effect of NPs on biological systems. The important property of the magnetic NPs that need to be address is that of biocompatibility with cell lines i.e. to investigate cytotoxicity.

Cytotoxicity:

Ferrite or iron oxide NPs are the most widely used electromagnetic materials, finding applications over a wide range due to their low cost and high performances [48]. Alternating magnetic field heats up the ferrite NPs, allowing its applications in imaging and therapy [45]. In the recent years the research has focused on evaluating cytotoxicity of ferrite/iron oxide NPs. It is found a cell-specific response to bare iron oxide nanoparticle exposure on cell lines [49]. 3T3 cells remained proliferative with the addition of up to 30 ppm iron oxide; however, human mesothelioma cells exhibited significant reduction in cell viability at only 3.75 ppm iron oxide. The tested higher concentrations of NPs (0-09-23.05mM) on COS -7 cell lines [50] and found no significant differences between the exposed cells and the control. It was found the effect of 0 - 250μg/ml bare iron oxide particles on Rat Liver cells BRL3A and found that there was 30% decrease in the cell viability [51]. The PEG-coated NPs were biocompatible with human fibroblast cells and showed more than 99% viability compared with the controls [52]. On the other hand, bare iron oxide NPs induced a 25–50% loss in fibroblast viability at 250 mg per ml. The effects of three surface coatings on iron oxide cytotoxicity and found MPEG– Asp3- NH2-coated iron oxide NPs had almost no

cytotoxicity at the concentrations tested [53]. In comparison, MPEG–PAA- and PAA coated iron oxide NPs significantly reduced cell viability with only 16% of the cell remaining at an iron concentration of 400 mg per ml. As bare iron oxide NPs adsorbed to the cell surface, cell counts after incubation indicated that uncoated iron oxide NPs also significantly reduced cell viability. This study was conducted on the OCTY mouse cell lines. In most of the studies the cytotoxicity was evaluated by viability and 3-(4,5-dimethyl-2-thiazolyl)-2,5-diphenyl-2H-tetrazolium bromide (MTT) assay. The studied interaction of magnetic microspheres with cells (adherent human prostate cells (DU- 145) and Murine suspension lymphoma cells (EL-4), using an in vitro 3-[4,5-dimethylthiazol-2yl]-2,5- diphenyltetrazolium bromide (MTT) assay [54]. Viability and metabolic activity were reduced in all examples. However, the MTT assay is not recommended for all cell lines due to high variability and non-specificity. So our preliminary test was on human lymphocyte cells to evaluate biocompatibility for getting optimum effect for drug delivery system. The cytotoxicity effects of iron oxide coated with thiol containing hydrophilic ligands has found to be non-toxic in human lymphocytes and nitric oxide releasing iron oxide NPs are found to be toxic in human lymphocytes [12], $CoFe_2O_4$ NPs found to be biocompatible with human lymphocyte cells [55]. In the present investigation, the synthesized uncoated and coated iron oxide based NPs biocompatible studies are evaluated on human lymphocyte cells by Trypan blue dye exclusion test. The in-vitro cytotoxicity studies of the NPs using different cell lines are increasingly published. However, these studies include a wide range of NPs concentration and exposure time, making it difficult to determine whether the cytotoxicity observed is physiologically relevant. The disparity in the results obtained by the various assays could be because of the culture condition, incubation time, concentration of the NPs and the assays used for testing viability. The cytotoxicity pattern varies from one cell types to the other. The uptake of NPs into the organism often induces or suppresses some biological processes or activities. In our work we have investigated the effect of various magnetic NPs on the angiogenesis activity that is discussed below.

Cytotoxicity was analysed in terms of percentage of dead cells.The cell viability was determined by the following formula:

$$\%\ cell\ viability = \frac{No.of\ viable\ cells}{Total\ no.of\ cells}\ X\ 100$$

Angiogenesis activity

Angiogenesis is the physiological process through which formation of new blood vessels takes place from pre-existing vessels. This is distinct from vasculogenesis which is a biological process by which new blood vessels are formed from endothelial cells from mesoderm cell precursors [56]. The process of angiogenesis is controlled by chemical signals in the body. These signals can stimulate both the repair of damaged blood vessels and the formation of new blood vessels. Other chemical signals, called angiogenesis inhibitors, interfere with blood vessel formation. Normally, the stimulating and inhibiting effects of these chemical signals are balanced so that blood vessels are formed only when and where they are needed [57]. Angiogenesis plays a key role in various physiological and pathological conditions, including embryonic development, wound repair, inflammation and tumor growth [58]. Angiogenesis is important for normal growth and wound healing processes. An imbalance of the growth factors involved in this process causes impairment of angiogenesis and is associated with several diseases such as diabetes mellitus, malignant, ocular and inflammatory diseases. In diabetes mellitus, delayed wound healing is due to defective angiogenesis. There are many models to study the angiogenesis activity such as mouse model and Chick Chorioallantoic membrane model. Chick Chorioallantoic membranes (CAM) from developing chick eggs are routinely used in biological and biomedical research. To investigate development of angiogenesis, tumors and propagate to investigate viruses or helminthes [59-65]. CAM model is more used because of its extensive vascularization, low cost, easy accessibility, reliability and reproductively. The CAM has been broadly used to study the morph functional aspects of the angiogenesis process in vivo and to investigate the efficacy and mechanism of action of proangiogenic and antiangiogenic natural and synthetic molecules [66, 68]. Recently it has found that dextran hydrogel scaffolds enhance angiogenic responses and promote complete skin regeneration during burn wound healing [65], fluorescein isothiocyanate (FITC)-dextran is used to enhance angiogenesis activity in mice [69], chitosan encapsulated loaded zinc ferrite for biocompatible drug delivery on chicken embryonic stem cells [70], uncoated ferrite NPs used in modulation of angiogenesis activity in Chick chorioallantoic membrane (CAM) [71], biogenic silver nanoparticle synthesized using saliva shows anti-angiogenesis effect in (CAM) [72]. Gold and silver NPs conjugated with heparin derivative possess anti-angiogenesis properties in (CAM) assay [73]. Carbon materials such as graphites, multiwalled carbon nanotubes and fullerenes inhibit vascular endothelial growth factor and fibroblast growth factor promoted angiogenesis [74].

Amine functionalized MFe_2O_4 (M = Co, Ni and Mn) promotes angiogenesis in (CAM) [75]. Gold and Silver NPs are found to be anti-angiogenesis properties in CAM, while iron oxide NPs are found to be angiogenenic properties in CAM [71, 73, 75]. There are not much reported data on iron oxide NPs as stimulate angiogenesis activity.

Angiogenesis activity in CAM

The Effect of the NPs on angiogenesis was evaluated using Chick Chorioalantoic membrane model (CAM). Three-day-old white chick leg horn eggs were purchased from Central Poultry Organisation Goregaon, Mumbai. The eggs were cleaned with ethanol and were incubated at 37^{o}C. On the fifth day, the eggs were inoculated with the test samples dispersed in saline through a tiny window in the eggshell and sealed with parafilm. The eggs were incubated at 37^{o}C. On the 14th day the eggs were broken gently from the site of air sac, and embryo was separated to expose the CAM. CAM was observed under stereo microscope and photographed using 8 megapixel camera at a fixed distance for all the cases. Blood vessels were counted to assign a score for the extent of angiogenesis based on the branching of vessels from the main vessel and sprouting of the branched vessels.

To estimate haemoglobin content, CAM was isolated, homogenized for 5 minutes and dispensed in 15ml of Drabkin's reagent. The solution with CAM was further centrifuged at 1500 rpm for 20 minutes. The supernatant was separated and readings were taken spectrophotometrically at 570 nm. When blood is treated with the Drabkin's reagent which contains potassium ferricyanide, potassium cyanide and $NaHCO_3$, haemoglobin reacts with ferricyanide to from met-haemoglobin and then reacts with cyanide to form cyan met-haemoglobin. The colour intensity of the product measured at 570 nm is proportional to the concentration of haemoglobin.

The conversion of optical density into Hemoglobin level in terms of g/dL is carried out as follows: The hemoglobin level (g/dL) was determined by the following formula for 1ml of Drabkin's reagent:

$$Hb\ \left(\frac{gms}{dL}\right) = \frac{O.D.of\ test}{O.D.of\ standard}\ X\ 15.06$$

O.D of test = Optical Density of test (iron oxide based NPs)

O.D of Standard = Optical Density of Standard hemoglobin

Eggs were treated in the study including 6 eggs (n=6) for each test concentration of the NPs.

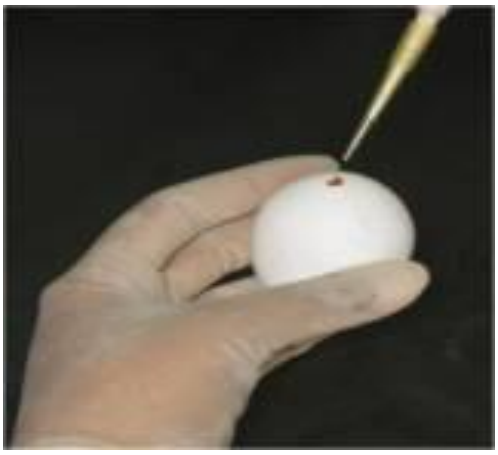

Figure 4. Inoculation of drug through open window on day 5.

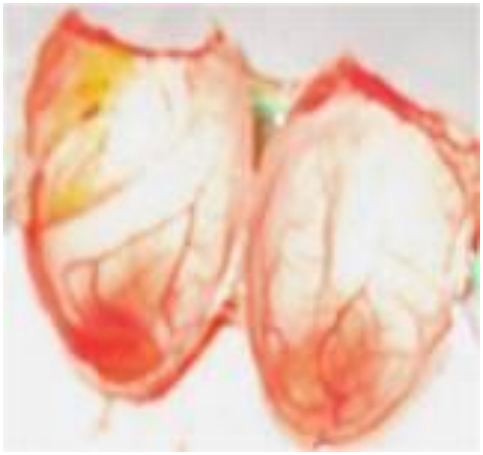

Figure 5. Isolation of CAM on day 14.

Statistical analysis was carried out using standard methods for calculating mean, Standard Deviations (S.D.) and Student's t-test and ANOVA test etc.

In this study, we used Student's t-test because the sample size is small (N<100). The cell viability and angiogenesis activity in CAM model for finding the effect of synthesized NPs before and after adding the NPs. The test whether hypothesis is accepted or rejected in terms of p-value/t-value: these indicators are calculated from the standard statistical formulae.

The formula for finding the t value is

$$t = \frac{X_{mean} - \ hypothesis\ value}{\frac{S_d}{\sqrt{n}}}$$

Where X_{mean} is mean of difference, hypothesis value = 0, S_d = Standard deviation and n = no. of population.

The t-value and p-values were calculated using Microsoft excel spreadsheets

Magnetic Resonance Imaging (MRI) Contrast agents:

Magnetic Resonance Imaging (MRI) has been developed using the principles of nuclear magnetic resonance. This is a powerful tool for detailed virtualization of body internal of body internal structure. It gives an opportunity to visualize soft tissues, to detect physiological and chemical changes in organism. MRI is a diagnostic technique based on interactions between protons of human body and powerful magnetic field. Due to water percentage of our body is approximately 80%, hydrogen nucleus (protons) with unpaired spins work as a great instrument influenced by external magnetic field. Spins precess along an axis of exposed magnetic field with the frequency, called precessional frequency, or Larmor frequency:

$$\omega_o = \gamma B_o$$

where ω_o is the recessional frequency, γ is the gyromagnetic ratio (ratio of the magnetic moment to the angular moment of definite system, in our case is proton), B_o is a magnetic flux density. When perpendicular to magnetic field precessional frequency (in radiofrequency range) impulse is applied, magnetic resonance phenomena occur- protons absorb energy and transfer from stable initial state to unstable excited state. After removal of Larmor frequency pulse, the excited spins realign to equilibrium state parallel with B_o and radiate absorbed before energy. This phenomenon is named spin relaxation. Due to protons from different tissues possess different relaxation values, there are differences between signals which are used to construct the image of organism`s anatomy. Proton signals are registered and interpreted via a mathematical algorithm to a graphical view [76-79]. The applications of NPs in medicine has led to the use of Superparamagnetic iron oxide nanoparticles (SPIONs) for therapeutic uses as magnetically guided drug delivery systems for treatment of cancer and for diagnostic purposes such as Magnetic Resonance Imaging (MRI) contrast agents [80]. The strength of MRI is its excellent discrimination between soft tissues, providing naturally the contrast between the structural differences of normal and pathological tissues. This visibility of internal body structures and contrast is further enhanced by the use of MRI contrast agents. The role of contrast agents in MRI is very important. There are two types of relaxation in MRI with times T_1 and T_2, which occur simultaneously, independent of each other. The longitudinal T_1 relaxation time of water exhibit bright or positive contrast whereas transverse T_2 relaxation time of water produces dark or negative contrast. Relaxivitiy is a measure of the ability of MRI contrast agents to increase the relaxation of the surrounding nuclear spins (hydrogen protons), which can then be used to improve the contrast in MR images. Relaxivity is expressed in units of $mM^{-1}s^{-1}$ of NPs. The contribution of paramagnetic contrast agents to the relaxation of

the nuclear spins is due to both the inner and outer sphere processes. The inner sphere process is due to the chemical interchange interaction between the bond water of the paramagnetic agents and the surrounding free water, which eventually increases the relaxation (larger effect on T_1) of nuclear spins. In contrast the outer sphere process occurs when the paramagnetic agents diffuse through free water. In this process, random fluctuations of paramagnetic agents create a local magnetic field of paramagnetic agents create a local magnetic field inhomogeneity, thus increasing the relaxation (larger effect on T_2) of nuclear spins [81, 82]. In the clinically used gadolinium-based contrast agents, gadolinium ions are formed as chelates. Thus, the bound water of the chelates can continuously interact with the surrounding free water and increase the T_2 relaxation of nuclear spins. Most gadolinium chelate agents have an inner sphere effect that is greater than the outer sphere effect; therefore, they are used as T_1 contrast agents. Coated ferrite nanoparticle agents, however, are completely surrounded by their coating material, and the chemical interchange interaction (inner sphere process) does not occur. In addition, the ferrites NPs have a much larger magnetic moment than gadolinium ions and produce larger magnetic field fluctuations (inhomogeneity). Due to this property of magnetic NPs, they are considered to be ideal T_2 contrast agents [82]. So contrast agents are classified as T_1 (positive) agents and T_2 (negative) agents. The process of imaging at high field (9 Tesla) and frequencies have been found to produce undesirable side effects in patients and techniques of imaging are developed to produce better resolution at moderate fields. This has been achieved by the use of suitable magnetic contrast agents with the ability to modulate the T_1 and T_2 relaxivities. These imaging techniques adopted T_1 and T_2 weighted sequences, depending on the tissues to be scanned. Currently, the conventional media used were paramagnetic gadolinium based agents are used for T_1-weighted image that are relatively expensive and superparamagnetic iron oxide based magnetic NPs used for T_2-weighted image [83-87]. The conventional T_1 MRI contrast agents have heavy metals like Gd that are paramagnetic; there have been reports that these heavy elements leave traces in the brain over a long period of time. Hence there is a need to consider materials that are relatively safe and hence we have conducted a study on iron oxide based NP formulations which are relatively safe and non-toxic. The quality of MRI images depends upon the several parameters such as applied magnetic field, radio frequency, the proton spin density, the nuclear spinlattice relaxation time T_1, the spin-spin relaxation time T_2, contrast agents and nature of the tissues to be scanned [88-90]. T_1-weighted scanning shows fat brighter but water darker and are called positive; T_2-weighted scanning shows

reverse – fat darker and water brighter, so called negative. T_1 sequence is more efficient for brain imaging, T_2 for spinal cord diagnostics [91].

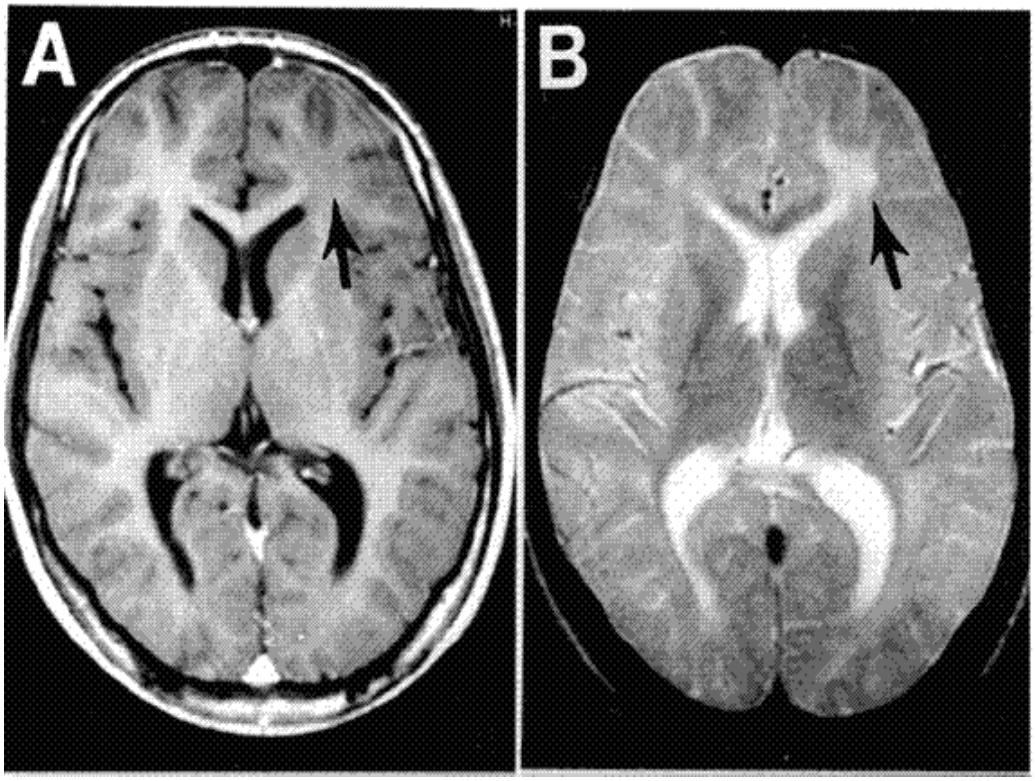

Figure 6. T_1 (A) AND T_2 (B) weighted images of human brain [89]

The SPIONs used as MRI T_2 contrast agents must have combined properties of high magnetic saturation, size less than 50 nm, biocompatibility, pH neutrality, chemical stability and agglomeration free. The SPIONs used as MRI T_2 contrast agents must have combined properties of high magnetic saturation, size less than 50 nm, biocompatibility, pH neutral, chemical stability and agglomeration free. The main problem with SPIONs is their fast agglomeration in water due to the high surface to volume ratio and magnetization. To reduce agglomeration these NPs are coated with various polymers such as dextran, chitosan, polyethylene glycol (PEG), polyvinyl alcohol (PVA) etc. to enhance biocompatibility, and longer shelf life and are successfully used as MRI contrast agents [92-95]. There are various reported literature on SPIONs used as MRI T_2 contrast agents that includes uniform mesoporous silica coated with iron oxide NPs as MRI T_2

contrast agents [96], chitosan coated SPIONs used as MRI contrast agents in vivo [97], folic acid conjugated glucose and dextran coated iron oxide NPs as MRI contrast agents [98], polyvinyl pyrrolidone (PVP) functionalized SPIONs used as MRI contrast agents [99], amine functionalized iron oxide NPs for T_2 contrast agents [100] and Manganese ferrite NPs conjugated with gadolinium and folic acid for dual contrast T_1 and T_2-weighted MR images in hela cells [101]. Therefore challenge in these areas is to synthesize high quality aqueous iron oxide NPs and should be biocompatible which can give improved relaxation compared to the existing commercial MRI contrast agents [102].

In the present thesis, we have synthesized a series of such Ferrite NPs both uncoated and coated with different organic, inorganic and polymer materials, by various chemical synthetic procedures. They have been characterized by various complementary techniques that are briefly discussed. The test for biocompatibility has been carried out in vitro on cell lines of human lymphocytes. The applicability of these formulations as T_2 MRI contrast agents was examined on a clinical MRI machine. The effect of the NP formulations into the chick chorioallantoic membrane (CAM) of fertile leghorn chick eggs was examined in-vitro for studying the bioactivity of angiogenesis that deals with the formation of new blood vessels from pre-existing vessels.

Scope of study:

The recent research interest in magnetic NPs is stimulated by a variety of potential applications of these materials, ranging from soft to hard magnetic materials and from ultra-high density information storage to biomedical applications. Since contrast agents are used in magnetic resonance imaging (MRI), numerous efforts have been undertaken to increase their relaxivity. Several Iron oxide based NPs and related formulations are identified as T_2 MRI contrast agents. Iron oxide based NPs have to meet several specifications in order to be applied T_2 MRI contrast agents. Important features of these NPs are that they should have are a small overall size, superparamagnetism, high colloidal stability in water, (ie the NPs suspension in water does not settle down when large field is applied) and biocompatibility both for*in vitro* and *in vivo* applications. Comparative studies of synthesis and characterization of iron oxide based NPs are carried out. The cytotoxicity of the synthesized NPs with lymphocytes and their use as T_2 contrast agents in MRI was investigated.

MRI measurement:

The T_2 relaxation times (sec) measurement was done using a 3T clinical MR Scanner (General Electric Healthcare, USA). Samples of different concentrations of magnetic NPs were prepared by diluting them with distilled water for aqueous solutions and Minimum Essential Medium (MEM) for cells. T_2 weighted images were obtained with a multiple fast spin echo pulse (FSE) sequence (repetition time T_R = 3500 ms; echo time T_E = 15, 30, 45, 60, 75 and 90 ms; matrix 512 x 512). For MRI analysis the aqueous solution of magnetic NPs are taken in Elisa plate i.e. (0.2, 0.1. 0.08, 0.04, 0.02, 0.01, 0.005 and 0 mM) and treated with human lymphocyte cells i.e. (0.4, 0.2, 0.16, 0.08, 0.04, 0.02, 0.01 and 0 mM) at eight different Fe concentrations. The Fe concentration used for NPs treated with lymphocyte cells are twice to those of aqueous solutions (untreated with cells). The image obtained from MRI machine is in Dicom file and is converted into jpeg or tiff format by RadiAnt Dicom viewer software. The T_2 value is calculated by ImageJ MRI plugin calculator. The r_2 ($1/T_2$) relaxivity values in (mM^{-1} s^{-1}) were calculated from the slope of the linear plots of $1/T_2$ versus the Fe concentrations and the formula is given below:

$$\frac{\mathbf{1}}{\boldsymbol{T_2}} = \frac{\mathbf{1}}{\boldsymbol{T_2^o}} + \boldsymbol{r_2}[\boldsymbol{Fe}]$$

Where $1/T_2$ is the observed relaxation rate in the presence of iron oxide NPs. $1/T^o_2$ is the relaxation rate of pure water, [Fe] is the concentration of Fe ion, and r_2 ($1/T_2$) is the transverse relaxation rate [103].

Conclusions:

The present study was aimed at discuss in detail methods commonly used in synthesis of magnetic nanoparticles (NPs) with various coatings and characterization with XRD, Raman spectroscopy, FTIR, UV-Visible Spectroscopy, BET, DLS, magnetization and SEM. The next step was to evaluate biocompatibility of NPs with human lymphocyte cells and study their effect of angiogenesis activity in CAM model. The intended application as MRI contrast agents of the NPs in aqueous has been studied in deep. The descriptive method for MRI to carry out on the lymphocyte cells incubated with NPs has been studied. In future scope, it is possible to design and develop applications based on these multifunctional properties eg. optofluidic, magneto-optic,

magneto-fluidic sensors and probes that can act as diagnostic and therapeutic probes, and is also termed as theranostic applications.

References:

1] Q. A. Pankhurst, J. Conolly, S. K. Jones and J Dobson, J. Phys. D: Appl. Phys. **36** (2003) R167-R181, *doi: 10.1088/0022-3727/36/13/201*

2] Y. Li, W. Kim, Y. Zhang, M. Rolandi, D Wang and H. Dai, J. Phys. Chem. B, **105** (2001) 11424-11431, *doi: 10.1021/jp012085b*

3] H W. Zhang, Y. Lui, S H. Sun, J. Frontiers of Phys in China. **5** (2010) 347-356, *doi: 10.1007/s11467-010-0104-9*

4] J R. Stephens, J S. Beveridge and M E. Williams, Phys. Chem. Chem. Phys. **14** (2012) 3280-3289, *doi: 10.1039/c2cp22982j*

5] R. Y. Hong, T. T. Pan, Y. P. Han, H. Z. Li, J. Ding, H. Sijin, J. Magn. Magn. Mater. **310** (2007) 37-47, *doi: 10.1016/j.jmmm.2006.07.026*

6] A. S. Arbab, L. A. Bashaw, B. R. Miller, E. K. Jordan, B. K. Lewis, H. Kalish, H. J. A. Frank, Radiology. **229** (2003) 838-846, *DOI: http://dx.doi.org/10.1148/radiol.2293021215*

7] C. Sun, C. Fang, Z. Stephen, O. Veiseh, S. Hansen, D. Lee, R. G. Ellenbogen, J. Olson, M. Zhang, Nanomedicine (Lond). **3** (2008) 495-505, *doi: 10.2217/17435889.3.4.495*

8] R. Y. Hong, B. Feng, L. L. Chen, G. H. Liu, H. Z. Li, Y. Zhang and D. G. We, Biochem. Eng. J. **42** (2008) 290-300, *doi: 10.1016/j.bej.2008.07.009*

9] G. Y. Li, Y. Jiang, K. Huang, P. Ding and P. Chen, J. Alloys. Comp. **466** (2008) 451-456, *doi: 10.1016/j.jallcom.2007.11.100*

10] A. B. Salunkhe, V. M. Khot, N. D. Thoral, M. R. Phadatare, C. I. Sathish, D. S. Dhawale and S. H. Pawar, App. Surface. Sci. **264** (2013) 598-604, *doi: 10.1016/j.apsusc.2012.10.073*

11] A. Mukhopadhyay, N. Joshi, K. D. Chattopadhyay and G. A. Facile, App. Mater. Interfaces. **4** (2012) 142-149, *http://dx.doi.org/10.1021/am201166m*

12] R de Lima, JL de Oliveira, A. Ludescher, MM. Molina, R. Itri, AB. Seabra and PS. Haddad, Journal of Phys: Conference Series. **429** (2013) 1-7, *doi:10.1088/1742-6596/429/1/012034*

13] S. F. Shi, J. F. Jia, X. K. Guo, Y. P. Zhao, D. S. Chen, Y. Y. Gou, T. Cheng, X. Y. Zheng, Int. J. NanoMedicine. **7** (2012) 5593-5602, *doi: 10.2147/IJN.S34348*

14] J. Sun, S. Zhou, P. Hou, Y. Yang, J. Weng, X. Li, M. Li. J. Biomed. Material Research Part A. **80A** (2007) 333-341, *doi: 10.1002/jbm.a.30909*

15] C. M. Hurd, "Varieties of magnetic order in solids", CONTEMP. PHYS. **23** (1982) 469-493, *http://dx.doi.org/1010.1080/00107518208237096*

16] C. D. Stanciu, A. V. Kimel, F. Hansteen, A. Tsukamoto, A. Itoh, A. Kirilyuk and Th. Rasing, Phys. Rev. B, **73** (2006) 220402(R), *doi: 10.1103/PhysRevB.73.220402*

17] B. D. Cullity, Introduction to Magnetic Materials, Addison -Wesley, MA (1972)

18] J. Frenkel, J. Doefman: Nature, **126** (1930) 274-275, *doi: 10.1038/126274a0*

19] C. P. Bean, J. D. Livingston, J. Appl. Phys, Supplement to **30 (4)** (1959) 120S-129S, *http://dx.doi.org/10.1063/1.2185850*

20] L. Neel, Ann. Geophys. **5** (1949) 99-136.

21] L. Neel, CR Acad. Sci. **252** (1961) 4075-4080

22] L. Neel (Eures Scientifiques (1978) Editions du CNRS Paris English translation: Selected works of Louis Neel (1988) Gordon & Breach, Sci - Publishers, New York, London.

23] P. Patnaik, Dean's Analytical Chemistry Handbook, 2nd ed. McGraw-Hill, 2004.

24] D. Harvey, Modern Analytical Chemistry, McGraw-Hill (2000). *ISBN: 10 0-7141060-0*

25] A. H. Li, E. L. Salabas and F. Schuth, Angrew. Chem., Int. Ed., **46** (2007) 1222-1244, *doi: 10.1002/anie.200602866*

26] G. Gnanaprakash, S. Ayyappan, T. Jayakumar, John Philip and Baldev Raj, Nanotechnology, **17** (2006) 17: 5851-5857, *doi:10.1088/0957-4484/17/23/023*

27] G. Gnanaprakash, John Philip, T. Jayakumar and Baldev Raj J. Phys. Chem. B, **111** (2007) 7978-7986, *doi: 10.1021/jp071299b*

28] S. Ayyappan, John Philip and Baldev Raj, J. Phys. Chem. C, **113** (2009) 590-596, *doi: 10.1021/jp8083875*

29] S. Ayyappan, S. Mahadevan, P. Chandramohan, M. P. Srinivasan, John & Philip and Baldev Raj, J. Phys. Chem. C, **114** (2010) 6334-6341, *doi: 10.1021/jp9.11966p*

30] M. A. Willard, L. K. Carpenter, E. E. Calvin, S. Calvin, V. G. Harris, Int. Mater. Rev. **49** (2004) 125-170, *doi: 10.1179/09506004225021882*

31] I. J. Bruce, J. Taylor, M. Todd, M. J. Davies, E. Borioni, C. Sangregorio, T. Sen, J. Magn. Magn. Mater. **284** (2004) 145-160, *doi: 10.1016/j.jmmm.2004.06.051*

32] S. Khalafalla, G. Riemers, IEEE Trans. Magn. **16 (2)** (1980) 178-183, *doi: 10.1109/TMAG.1980.1060578*

33] L. Babes, B. Denizot, G. Tanguy, J. J. Le Jeune, P. Jallet, J. Colloid Interface. **212** (1999) 474-482.

34] J. Park, K. An, Y. Hwang, J-G. Park, H-J. Noh, J-Y. Kim, J-H Park, N-M. Hwang, T. Hyeon, Nat. Mater. **3** (2004) 891-895., *doi: 10.1038/nmat1251*

35] P. Tartaj, M. P. Morales, S. Veintemillas-Verdaguer, T. Gonzalez-Carreno, C. J. Serna, Handbook of Magnetic Materials, **9** (2006) 403-533, *doi: 10.1016/S1567-2719(05) 16005-3*

36] Y. Li, M. Afzaal, P. O'Brien, J. Mater. Chem. **16** (2006) 2175-2180, *doi: 10.1039/B517351E*

37] A. Domortiere, P. Panissod, B. P. Pichon, G. Pourroy, D. Guillon, B. Donnio, S. Begin-Colin, Nanoscale, **3** (2011) 225-232, *doi: 10.1039/c0nr00521e*

38] S. F. Chin, S. C. Pang, C. H. Tan., J. Mater. Environ. Sci. **2** (2011) 329-302, *ISSN: 2028-2508*

39] S. L. Peshkovsky,and A. S. Peshkovsky, , Ultrason. Sonochem., **14** (2007) 314–322, *doi:10.1016/j.ultsonch.200607.003*

40] A.S. Peshkovsky and S.L. Peshkovsky, Sonochemistry: Theory, Reactions and Syntheses, and Applications, Hauppauge, NY: Nova Science Publishers (2010)

41] A.S. Peshkovsky and S.L. Peshkovsky, Book Series: Physics Research and Technology, Hauppauge, NY: Nova Science Publishers (2010)

42] K. S. Suslick, "Sonochemistry", Science **247** (1990) 1439-1990, *doi: 10.1126/science247.4949.1439.*

43] K. S. Suslick and D. J. Flannigan, Annual Rev. Phys. Chem. **59** (2008) 659-683, *doi: 10.1146/annurev.physchem.59.032607.093739*

44] K. S. Suslick and S. Kenneth , The Chemical Effects of Ultrasound, Scientific American, (1989) 62-68.

45] N. Lewinski, V. Colvin, and R. Drezek "Cytotoxicity of Nanoparticles" Wiley-VCH Verlag GmbH&Co. KGaA, Weinheim , Small, **4** (2008) 26 -49 *doi: 10.1002/smll.200700595*

46] Zhao, X., Hilliard, L. R., Wang, K., and Tan, W. (2004) Bioconjugated silica nanoparticles for bioanalysis. In Encyclopedia of Nanoscience and Nanotechnology (Nalwa, H. S., Ed.) pp 255–268, American Scientific Publishers, Stevenson Ranch. 4

47] Kairemo Kalveli, Paola Erba, Kim Bergstrom and Ernest K.J. Pauwels; “Nanoparticles in cancer”, **1** (2008) 30-36.

48] J. Wang, P. F. Chong, S. C. Ng, L. M. Gan, Mater. Lett. **30** (1997) 217-221, *doi: 10.1016/S0167-577X(96)00200-5*

49] T. Brunner, P. Wick, P. Manser, P. Spohn, R. Grass, L. Limbach, A. Bruinink, W. Stark, Environ. Sci. Technol. **40** (2006) 4374 – 4381.

50] F. Y. Cheng, C. H. Su, Y. S. Yang, C. S. Yeh, C. Y. Tsai, C. L. Wu, M. T. Wu, D. B. Shieh, Biomaterials, **26** (2005) 729–38,*doi: 10.1016/j.biomoterials.2004.03.016*

51] S. M. Hussain, K. L. Hess, J. M. Gearhart, K. T. Geiss, J. J. Schlager, Toxicol. In Vitro, **19** (2005) 975–983, *doi: 10.1016/j.tiv.2005.06.034*

52] A. K. Gupta, S. Wells, IEEE Trans. Nanobiosci. **3** (2004) 66–73.

53] S. Wan, J. Huang, M. Guo, H. Zhang, Y. Cao, H. Yan, K. Liu, J. Biomed. Mat. Res. Part A. **80A** (2007)946–954, *doi: 10.1002/jbm.a.31022*

54] Hafeli U.O, Gayle J. Pauer, “In vitro and in vivo toxicity of magnetic microspheres”, Journal of Magnetism and Magnetic Materials, **194** (1999) 76-82

55] Nooris Momin, Aparna Deshmukh and Radha S, J. Nanoresearch, **34** (2015) 1-8, *doi: 10.4028/www.scientific.net/JNanoR.34.1*

56] W. Risau and I. Flamme, “Vasculogenesis”. Annual review cell and development biology, **11** (1995) 73-91, *doi: 10.1146/annurev.cb.11.110195.000445*

57] D. Hanahan and J. Folkman, Cell. **86** (1996)353-364, *doi: 10.1016/S0092-8674(00)80108-7*

58] P. Carmeliet and R. K. Jain, Nature. **407** (2000) 249-257, *doi:10.1038/35025220*

59] J. Wilting, H. Neeff and B. Christ. Cell Tissue Res., **297** (1999) 1-11.

60] P. Osbody, M. J. Oursler, T. Salino-Hugg and M. Krukowski, Ciba Found. Symp, **136** (1988) 108-124.

61] D. Rabitta, Int. Rev. Cell. Mol. Biol, **270** (2008) 181-224.

62] A. M. Cimpean, D. Ribatti, M. Raica, Angiogenesis, **11** (2008) 311-319, *doi: 10.1007/s10456-008-91171*

63] P. R. Woolcock, Methods Mol. Biol. **436** (2008) 35-46, *doi: 10.1007/978-1-59745-279-3_6*

64] J. S. Guy, Methods Mol. Biol. **454** (2008) 109-117.

65] B. Fried and L. T. Stablefor, Adv. Parasitol. **30** (1991) 108-165.

66] D. Rabitti, Methods Mol. Biol, **843** (2012) 47-57, *doi: 10.1007/978-1-61779-523-7_5*

67] R. W. Cole, F. Liu and B. J. Herron, Microscopy: Science, Technology, Applications and Education, (2010) 885-896.

68] G. Sun, X. Zhang, Y. Shen, R. Sebastain, L. E. Dickinson, K. F. Talbot, M. Reinblatt, C. Steenbergen, J. W. Harmon and S. Gerecht, Prooceedings of the National Academy of Sciences of the United States of America **108** (2011) 20976-20981, *doi: 10.1073/pnas.1115973108*

69] L. Guedez, A. M. Rivera, R. Salloum, M. L. Miller, J. J. Diegmueller, P. M. Bungay and W. G. Stetler-Stevenson , American Journal of Pathology, **162** (2003) 1431-1439, *doi: 10.1016/S0002-9440(10)64276-9*

70] V. J. Sawant, S. R. Bamane and S. M. Pachchapurkar, Der Chemica Sinica, **4** (2013) 67-78. *ISSN: 0976-8505*

71] Aparna Deshmukh, S. Radha, Y. Khan and Priya Tilak, AIP Conf. Proc. **1349** (2011) 437-438, *doi: 10.1063/1.3605922*

72] J. Baharara, F. Namvar, M. Mousavi, T. Ramezani and R. Mohamad, Molecules, **19** (2014) 13498-13508. *doi: 10.3390/molecules190913498*

73] M. M. Kemp, A. Kumar, S. Mousa, E. Dyskin, M. Yalcin, P. Ajayan, R. J. Linhardt and S. A. Mousa, Nanotechnology **20** (2009) 1-7, *doi: 10.1088/0957-4484/20/45/455104*

74] S. Murugesan, S. A. Mousa, L.J. Connor, D. W. Lincoln and R. J. Linhardt, FEBS Letters. **581** (2007) 1157-1160. *doi: 10.1016/j.febslet.2007.02.022*

75] Nooris Momin, Aparna Deshmukh and Radha S, European BioPhys. J. (2015) 1-10, doi: *10.1007/s00249-015-1083-0*

76] R. H. Hashemi, W. G. Bradley, C. J. Lisanti, J. Magn. Reso. Imag. **7** (1997) 614-615.

77] M. P. Hiorns, Pediatr Nephrol, **26** (2011) 59-68, *doi: 10.1007/s00467-010-1645-4*

78] D. Formica and S. Silvestri, Bio. Med. Eng. **3** (2004) 1-12, *doi: 10.1186/1475-925X-3-11*

79] J. P. Ridgway, Journal of Cardiovascular Magnetic Resonance, **12** (2010**)** 7-15, *doi: 10.1186/1532-429X-12-71*

80] C. Sun, C. Fang, Z. Stephen, O. Veiseh, S. Hansen, D. Lee, R. G. Ellenbogen, J. Olson and M. Zhang, Nanomedicine (Lond)., **3** (2008) 495-505, *doi: 10.2217/17435889.3.4.495*

81] T. Ahmad, H. Bae, Y. Iqbal, I. Rhee, S. Hong, Y. Chang, J. Lee, D. Sohn, J. Magn. Magn. Mater. **381** (2015) 151-157, *doi: 10.1016/j.jmmm.201412.077*

82] R. B. Lauffer, Chem. Rev. **87** (1987) 901-927, *doi: 10.1021/cr00081a003*

83] P. Caravan, J. J. Ellison, T. J Mc Murry, and R. B. Lauffer, Chem. Rev., **99** (1999) 2293-2352, *doi: 10.1021/cr980440x*

84] C. Wilhelm, F. Gazeau, Biomaterials, **29** (2008), 3161-3174, *doi: 10.1016/j.biomaterials.2008.04.016*

85] B. Chertok, B. A. Moffat, A. E. david, F. Yu, Bergemann C, B. D. Ross, V. C. Yang, Biomaterials., **29** (2008) 487-496, *doi: 10.1016/j.biomaterials2007.08.050*

86] N. Nasongkla, E. Bey, J. Ren, H. Ai, C. Khemtong, J. S. Guthi, S. F. Chin, A. D. Sherry, D. A. Boothman, J. Gao. Nano Lett., **6** (2006) 2427-2430, *doi: 10.1021/nl061412u*

87] J. Wang, B. L. Zhang, G. yang, L. Wang, S. B. Xie, L. Xuan, F. B. Gao, Journal of inorganic materials., **30** (2015) 53-58, *doi: 10.15541/jim20140178*

88] M. G. Landsberg, M. Straka, S. Kemp et al., Lancet Neurology., **11** (2012) 860-867, *doi: 10.1016/S1474-4422(12)70203-X*

89] D. E. Sosnovik, M. Nahrendorf and R. Weissleder, Circulation, **115** (2007) 2076-2086, *doi: 10.1161/CIRCULATIONAHA,.106.658930*

90] P. V. Prasad, AJP Renal Physiology, **290** (2006) F958-F974, *doi: 10.1152/ajprenal.001142005*

91] W. P. Dillon, Neuroimaging in Neurologic Disorders, *Harrison's Principles of Internal Medicine*, 17th Edi. (**2008**) 2491-2497. *ISSN-13: 978-0071466332*

92] H. T. Chan, Y. Y. Do, P.L. Huang, P.L. Chien, T. S. Chan, R.S. Liu, C. Y. Huang, S. Y. Yang, H.E. Horny. J. Magn. Magn. Mater., **304** (2006) 415-417.

93] M. Yu, S. Huang, K. J. Yu and A. M. Clyne. Int. J. Mol. Sci., **13** (2012) 5554-5570.

94] M. Mahdavi, M. B. Ahmad, M. J. Haron, F. Namvar, B. Nadi, M. Z. Ab Rahman and J. Amin. Molecules., **18** (2013) 7533-7548, *doi: 10.3390/molecules18077533*

95] S. F. Shi, J. F. Jia, X. K. Guo, Y. P. Zhao, D. S. Chen, Y. Y. Guo, T. Cheng and X. L. Zhang. Int. J. Nanomedicine., **7** (2012) 5593-5602, *doi: 10.2147/IJN.S34348*

96] F. Ye, S. Laurent, A. Fornara, L. Astolfi, J. qin, A. Roch, Alssandro Martini, S. M. Toprak, R. N. Muller and M. Muhammed. Contrast Media Mol. Imaging, **7** (2012) 460-468, *doi: 10.1002/cmmi1473*

97] A. M. Reddy, B. K. Kwak, H. J. Shim, C. Ahn, H. S. Lee, Y. J. Suh and E. S. Park. J. Korean Med Sci., **25** (2010) 211-219, DOI: *http://dx.doi.org/10.3346/jkms.2010.25.2.211*

98] F. Dai, M. Du, Y. Liu, G. Liu, Q. Liu and X. Zhang, J. Mater. Chem. B., **2** (2014) 2240-2247, *doi: 10.1039/c3tb21732a*

99] N. Arsalani H. Fattahi and M. Nazarpoor, eXPRESS Polymer Letters., **4** (2010) 329-338.

100] K. C. Barick, M. Aslam, Y. P. Lin, D. Bahadur, P. V. Prasad, P. Vinayak and P. Dravid. J. Mater. Chem., **19** (2009) 7023-7029, *doi: 10.1039/b911626e*

101] Z. Wang, J. Liu, T. Li, J. Liu and B. Wang. J. Mater. Chem. B., **2** (2014) 4748-4753, *doi: 10.1039/C4TB00342J*

102] F. Q. Hu, L. Wei, Z. Zhou, V. L. Ran, Z. Li and M. Y. Gao, Adv. Mater., **18** (2006) 2553-2556, *doi: 10.1002/adma.200600385*

103] J. Wan, W. Cai, X. Meng and E. Liu, Chem. Commun., (2007), 5004-5006, *doi: 10.1039/b712795b*